Influence of functionalized graphene on the bacterial and fungal diversity of *Vicia faba* rhizosphere soil

CHEN Zhi-wen[1,2,†], REN Jing[3,†], QIAO Jun[1,2,3,*], ZHAO Jian-guo[1,2,3,*], LI Jing-wei[1,2,3], LIU Ze-hui[1,3], LI Wei-jia[1,2], XING Bao-yan[1], ZHANG Jin[1,3], NIE Hui[1]

（1. *Engineering Research Center of Coal-based Ecological Carbon Sequestration Technology of the Ministry of Education*, *Shanxi Datong University*, *Datong*, 037009, *China*;
2. *Key Laboratory of Graphene Forestry Application of National Forest and Grass Administration*, *Shanxi Datong University*, *Datong*, 037009, *China*;
3. *School of Chemistry and Chemical Engineering*, *Shanxi Datong University*, *Datong*, 037009, *China*）

Abstract: The effect of functionalized graphene on the growth and development of *Vicia faba* L. was investigated by analyzing its impact on the composition and diversity of the microbial community in rhizosphere peat soil. Seedlings of *V. faba* planted in this peat soil were treated with either distilled water (CK) or 25 mg·L^{-1} (G25) of functionalized graphene solution. Results showed that the height and root length of *V. faba* seedlings in the G25 group were significantly larger than those in CK group. The microbial community was analyzed by amplifying and sequencing the 16S rRNA gene V3–V4 region of bacteria and internal transcribed spacer region of fungi in rhizosphere soil using Illumina MiSeq technology. Alpha and beta diversity analysis indicated that functionalized graphene increased the richness and diversity of bacteria and fungi in the *V. faba* rhizosphere peat soil. The abundances of three nitrogen cycling-related bacteria, *Hydrogenophaga*, *Sphingomonas* and *Nitrosomonadaceae*, were also altered after treatment with the functionalized graphene. The relative abundance of *Basilicum*, related to soil phosphorus solubilization, decreased in the fungal community, while the relative abundance of *Clonostachys* and *Dimorphospora*, which exhibited strong biological control over numerous fungal plant pathogens, nematodes and insects, increased in the soil after functionalized graphene treatment. Redundancy analysis revealed that the potential of hydrogen (pH), organic matter, and total phosphorus contributed the most to the changes in bacterial and fungal community composition in the rhizosphere soil. Overall, our findings suggested that the addition of functionalized graphene altered the relative abundances of nitrogen and phosphorus cycling-related microorganisms in peat soil, promoting changes in the physicochemical properties of the soil and ultimately leading to the improved growth of *V. faba* plants.

Key words: Functionalized graphene; *Vicia faba* L.; Plant growth; Rhizosphere soil; Microbial diversity

1 Introduction

Functionalized graphene has a large specific surface area, stable structure and excellent adsorption properties[1]. Due to these physicochemical properties, researchers are beginning to use functionalized graphene in agriculture, for example, as a retarder for potassium nitrate fertilizers or as a carrier for pesticides[2-3]. Kamal et al[4] discovered that functionalized graphene treatment accelerated the root and aboveground growth of seedlings in two plants, cotton (*Gossypium hirsutum*) and periwinkle (*Catharanthus roseus*), but did not explain the action mechanism of functionalized graphene to promote the growth of both plants.

So far, most research has focused on the effects of functionalized graphene on plant growth from the perspective of molecular or physiological data. For instance, a recent study showed that functionalized graphene enhanced root respiration, leading to increased plant root growth based on the transcriptome data[5]. In maize, treating the roots with 25 mg/L of functionalized graphene increased the levels of ammonium ions (NH_4^+) and potassium (K^+) in the rhizosphere soil, and upregulated the expression of nitrogen and potassium metabolism genes[6]. In tomato roots, functionalized graphene elevated the root auxin

Received date: 2023-06-02; **Revised date:** 2023-12-23
Corresponding author: QIAO Jun, Associate Professor. E-mail: qiaojun_nk@163.com;
ZHAO Jian-guo, Professor. E-mail: jianguozhao9150@163.com
Author introduction: †CHEN Zhi-wen and REN Jing contributed equally to this work.
Supplementary data associated with this article can be found in the online version.

content and induced the expression of root development-related genes[7]. Another study indicated that functionalized graphene could enhance the photosynthetic capacity of leaves, increase the yield and morphological characters of roots and leaves, improve the protein and amino acid contents of leaves in *Aloe vera*[8]. However, there is still no research on the mechanism of how functionalized graphene affects the activity or abundance of soil microorganisms to promote plant growth. Since soil microorganisms play a crucial role in the biochemical cycle of soil[9], it is necessary to investigate the effects of functionalized graphene on soil microbial community diversity before widespread use of functionalized graphene in agriculture.

Current studies on the effect of functionalized graphene on soil microbial communities are divided into 3 categories. (1) The first category explores the effect of functionalized graphene on soil microbial communities in the presence of heavy metal ions[10]. (2) the second category examines the effect of functionalized graphene on soil microorganisms after forming complexes with nanoparticles[11]. However, both of these types of studies are influenced by heavy metal ions and composites, making it difficult to determine the effect of functionalized graphene alone on soil microorganisms. (3) The third category investigates the effect of functionalized graphene on soil microbial communities under greenhouse conditions[12-14]. However, there have been no studies conducted on the impact of functionalized graphene on the diversity of plant rhizosphere soil microbial communities.

The entry of functionalized graphene into the soil environment inevitably has direct or indirect effects on soil microbial communities, changing the microbial community structure and function. Microbial community diversity is an important indicator of the impact of foreign materials on soil activity and metabolic capacity[15]. Therefore, it is important to study the effects of functionalized graphene on microbial community diversity in the rhizosphere soil of plants. Herein, we report the effects of functionalized graphene on the diversity and composition of microbial communities in *V. faba* rhizosphere soil, as well as its effects on soil physical and chemical properties. By exploring the relationship between changes in the rhizosphere soil microbial composition of *V. faba* and the growth status of the plants, the relationship between functionalized graphene, rhizosphere soil microbes, and physicochemical properties can be verified. This help us to explain the mechanism of functionalized graphene in promoting the growth and development of *V. faba* plants.

2 Materials and methods

2.1 Preparation and characterization of functionalized graphene

The functionalized graphene used in this study was prepared in-house through an electrochemical method. Briefly, graphite was used as both the anode and cathode, while distilled water was used as the electrolyte. The graphite electrode was electrolyzed and oxidized using high-frequency pulse current to obtain the functionalized graphene. The electrochemical electric field was used to insert external electrolyte ions into the layered materials in a way similar to liquid phase stripping. The electric field was applied to drive the intercalation of electrolyte molecules into the graphite cathode directly by an electrochemical route. Consequently, the spacing between graphite layers increased, and the van der Waals force between them decreased. In summary, functionalized graphene was obtained by electrochemically stripping graphite using a nonoxidizing method.

The characteristics of the functionalized graphene were analyzed using Raman spectroscopy (HORIBA, LabRAM HR Evolution). A Renishaw inVia Qontor with a 532 nm excitation laser was used to obtain the Raman spectra. The morphology of the functionalized graphene was examined using both scanning electron microscopy (SEM, TESCAN MAIA 3 LMH) and transmission electron microscopy (TEM, TecnaiG2F20 S-TWIN TMP). The C/O ratio of the functionalized graphene was determined using X-ray energy-dispersion spectroscopy (EDS) (OXFORD INSTRUMENTS, INCAx-act). XRD spectra were meas-

ured using a PAN-analytical X'Pert Pro diffractometer (Cu *K*α radiation between 2 and 702). The XPS spectra (C 1s and O 1s) were measured using an ADES-400 spectrometer (VG Scientific, UK) equipped with a hemispherical analyser, a scanning electron gun (Kimball Physics, model EGG-3101) and an X-ray excitation source.

2.2 Pretreatment of experiment

The *V. faba* seeds of the same size were divided into 2 groups: the blank group (CK) and the experimental group (G25), each containing 30 seeds, and the experiment was repeated 6 times. The seeds were planted in pots filled with peat soil. Distilled water and 25 $mg \cdot L^{-1}$ functionalized graphene solution was poured into the flowerpot at 6 pm every Sunday for 4 weeks. After 30 days, the peat soil in the pot was removed, and the soil attached to the roots was saved. Then, the rhizosphere soil samples were mixed in a large iron dish and divided into 4 parts. A portion of the soil samples were immediately frozen in liquid nitrogen and stored in a −80 °C refrigerator for soil microbial sequencing. The remaining soil samples were dried naturally and used to measure soil physicochemical properties.

2.3 Determination of plant height and root length of *V. faba*

The plant height of *V. faba* was measured using a ruler with a measuring range of 1 m, and the distance from the cotyledon node to the apical meristem was defined as plant height. The *V. faba* roots were washed carefully with deionized water, and the root morphology of *V. faba* was scanned using an Epson Perfection V850 Pro (Seiko Epson Corp., Tokyo, Japan) at 600 dpi. WinRHIZO 4.0 b software was used to analyze the scanned root images[16].

2.4 Determination of physicochemical properties of rhizosphere peat soil

To determine the soil properties, 10 g rhizosphere peat soil was weighed and dissolved in 25 mL of distilled water. The mixture was stirred for a minute and left for 30 min. After that, the pH value of the supernatant was measured using a calibrated pH meter (Thermo Orion, Waltham, MA, USA). The contents of ammonium nitrogen (AN), available potassium (AK) and available phosphorus (AP) were determined by soil nutrient rapid analyzer (TPY-8A)[17].

The contents of organic matter were determined with the following method. In detail, we first weighed 39.23 g of dried potassium dichromate and dissolved it in 600 mL of distilled water, then adjusted the volume to 1 L to obtain the required potassium dichromate solution. We next weighed 1.376 g of dried glucose into a beaker, and added a small amount of water to dissolve it. We then added 1 mL of concentrated sulfuric acid and adjusted the final volume to 100 mL to create the 0.5%-C standard solution. The standard solution was obtained by adding 2 mL of 0.5%-C standard solution to 1 mL of distilled water in a 100 mL beaker. Subsequently, 1 g of soil sample was added to a 100 mL beaker with 3 mL of distilled water and shook vigorously to create the solution to be tested. Finally, 10 mL of potassium dichromate solution and 10 mL of concentrated sulfuric acid were added to the above small beaker and shaken vigorously for 20 min, followed by the addition of 10 mL distilled water after which it was shaken again. After standing, 10 mL of supernatant was taken and the volume was set to 50 mL. A soil nutrient rapid meter was used to obtain the OM content.

Total nitrogen (TN) content in rhizosphere peat soil samples was measured using the soil total nitrogen assay (Kjeldahl method, HJ 717-2014)[18]. Total phosphorus (TP) content was measured using soil total phosphorus assay (NY/T 88-1988)[19]. The total potassium (TK) content was determined by soil total potassium assay (NY/T 87-1988)[20].

2.5 Microbiome sequencing and analysis

The HiPure soil DNA kit (D3142) produced by Guangzhou Meiji Biotechnology Co., Ltd. was used to extract 0.25 g of peat soil total DNA, and the purity and concentration of extracted DNA were detected by NanoDrop microspectrophotometer. The DNA was diluted with sterile water to a concentration of 1 ng/μL. Peat soil DNA was used as template for PCR reactions, and the specific primers 341F (5'-CCtacGGGNGGCWGCAG-3') and 806R (5'-GGac-

tachVGGGtatCTAat-3') were used to amplify the target region of prokaryotic 16S rRNA (V3-V4). The specific primers ITS1-F (5'-CTTGGtCATTTagaggaagtaa-3') and ITS2 (5'-GCTGCGTTCTTCATCGATGC-3') were used to amplify the internal gene spacer region (ITS) of fungal ribosomal RNA. The PCR reaction system was 50 μL. PCR thermal cycling conditions were denaturated at 95 °C for 5 min, followed by 30 cycles (95 °C/1 min, 60 °C/1 min, 72 °C/1 min) followed by a final extension at 72 °C for 7 min. The AMPure XP Beads were used for PCR product purification. Finally, the library was constructed and sequenced using the Illumina Novaseq 6000 PE250 mode.

2.6 Quality screening of sequencing data

The raw bacterial and fungal sequence reads were subjected to FASTP data quality control to remove sequences with high proportion of N and low quality in reads. Then the software FLASH (v 1.2.11)[21] was used to concatenate the original data, and the concatenated sequences were filtered by the software Trimmomatic (*v* 0.33)[22] to get high-quality tags sequences.

2.7 Species annotation and taxonomic analysis

Operational Taxonomic Units (OTU) were obtained by clustering the Clean Tags at the level of similarity ⩾97% using USEARCH (v 9.2.64)[23-24]. The RDP Classifier (V 2.2), Silva (Release132, http://www.arb-silva.de) database and Unite (Release 8.0, http://unite.ut.ee/) database were used to identify and annotate bacterial and fungal OTUs with the confidence threshold as 0.8. The community composition of each sample was counted at each level (phylum, class, order, family, genus, species)[25-27].

2.8 Diversity analysis and redundancy analysis of physicochemical properties

The inter-group Venn analysis was carried out in the R language software VennDiagram package (v 1.6.16)[28]. Sobs, Chao1, ACE, Shannon and Simpson index were calculated by QIIME (v 1.9.1) software[29]. The LefSe analysis was used to identify the significance of differences between the CK and treatment groups at each classification level[30]. Sobs represents the number of OTUs detected by sequencing, Chao1/ACE index mainly reflects the species richness information of samples, Shannon index comprehensively reflects the species richness and evenness, and the values of the 4 indices are proportional to the diversity. Principal Component analysis (PCA), similarity analysis (ANOSIM) and redundancy analysis (RDA) were performed in the R software Vegan package (v 2.5.3)[31]. Shannon index curves and rank abundance curves were plotted in the R language software ggplot2 package (v 2.2.1)[32].

3 Results and discussion

3.1 Characteristics of functionalized graphene

Functionalized graphene used in this study was characterized by different methods. Scanning electron microscopy was used to observe and analyze its surface morphology (Fig. 1a). The results showed that the functionalized graphene used in this paper presented a state of stacking and folding, with an obvious layered structure (Fig. 1a). The transmission electron microscopy (TEM) images indicated that the functionalized graphene had a sheet-like morphology with different transparencies (Fig. 1b). Dark areas indicate the thick stacking nanostructure of functionalized graphene layers and the higher transparency areas correspond to the thinner films of functionalized graphene layers (Fig. 1b). Both Raman spectroscopy and infrared spectroscopy were used to characterize the structure of functionalized graphene. Raman spectroscopy can characterize the defect state of functionalized graphene. As shown in Fig. 1c, the representative peak *D* and peak *G* of functionalized graphene was obvious[33]. The *G* peak generated by the stretching and farmoving of sp^2-hybridized atoms in carbon rings, appeared near 1 578 cm^{-1}, representing the ordered sp^2 bond structure[34]. The *D* peak, related to the sp^3 hybrid structure, was near 1 349 cm^{-1}, representing defects and amorphous structures at the edge of functionalized graphene[35]. The infrared spectrum was used to characterize the surface functional groups of functionalized graphene (Fig. 1d), showing that the functionalized graphene included different oxygen-

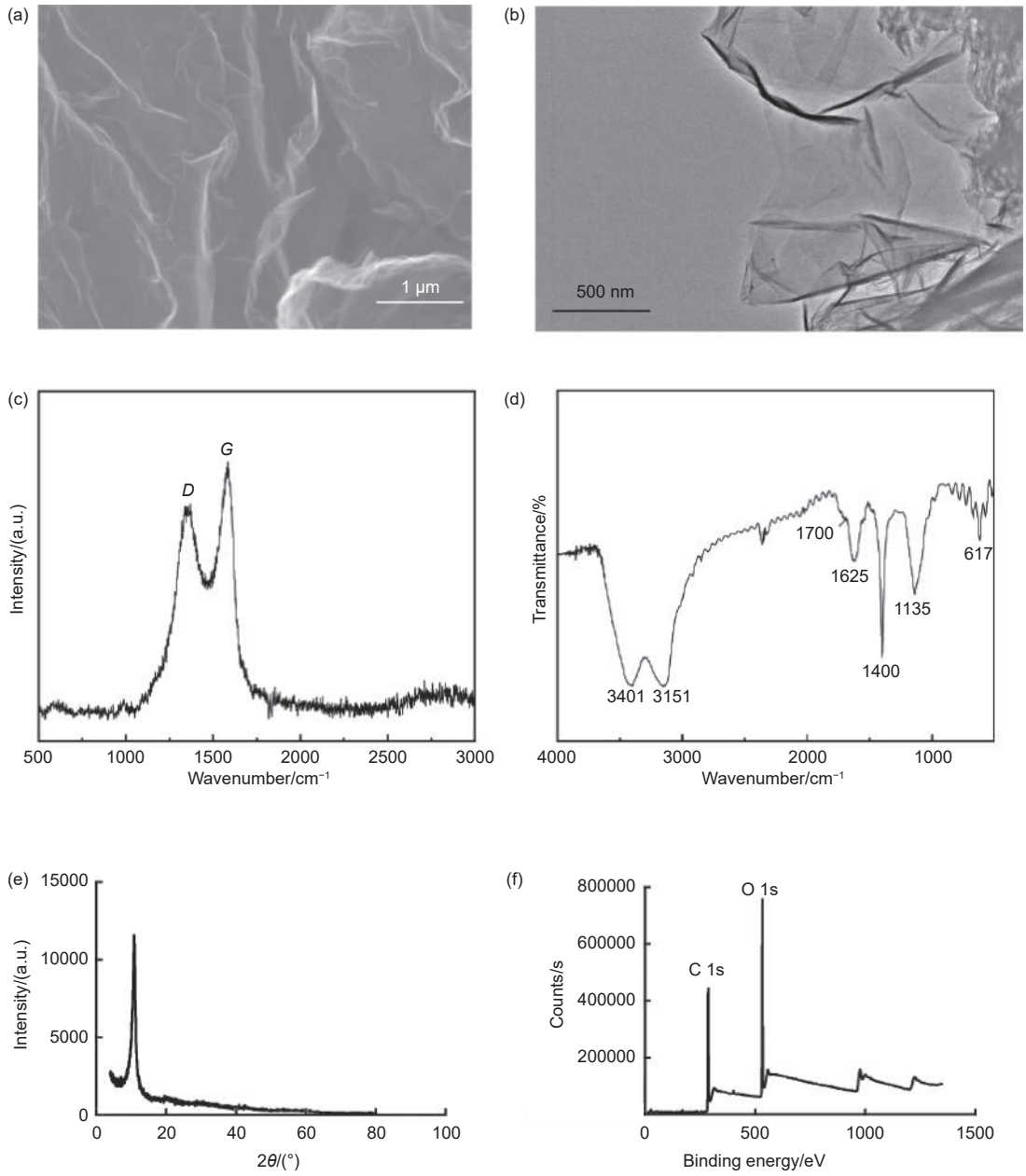

Fig. 1　Characterization of functionalized graphene. (a) SEM image, (b) TEM image, (c) Raman spectrum, (d) Fourier transform infrared (FT-IR) spectrum, (e) XRD curves of functionalized graphene, and (f) Results of C 1s and O 1s spectra fitting into C and O chemical groups for XPS spectrum

containing functional groups, including C—O (1 135 cm^{-1}), C—OH (1 400 cm^{-1}), C=C (1 625 cm^{-1}) and —OH (3 401 cm^{-1})[36]. The XRD pattern of functionalized graphene showed the characteristic peak for (002) crystal plane positioned at 2θ = 10.8° (Fig. 1e), indicating a short-range order[37]. The survey XPS spectra recorded from the functionalized graphene showed the carbon and oxygen at the surface (Fig. 1f). The prepared functionalized graphene samples showed a high content of oxygen (30.5%) with a C/O ratio about 7 : 3, which resulted from the analysis of the area under C 1s and O 1s spectra (Fig. 1f).

3.2　Functionalized graphene treatment promoted plant height and root development of *V. faba*

The phenotypes of *V. faba* plants were photographed after 30 days of treatment with distilled water and 25 $mg \cdot L^{-1}$ functionalized graphene solution, respectively (Fig. 2a). Fig. 2b showed that the plant height of *V. faba* significantly increased after functionalized graphene treatment (t = 2.246, P<0.05). In addition, the root phenotype of *V. faba* was also pho-

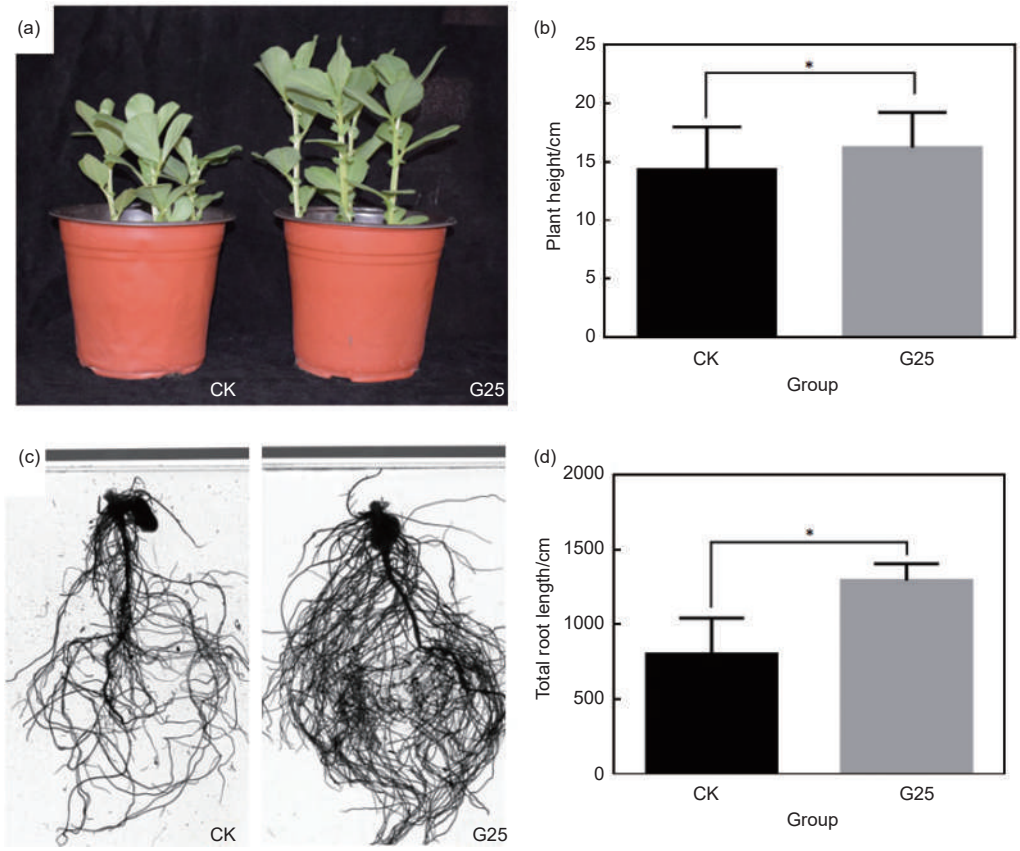

Fig. 2 Growth state of *V. faba* treated with functionalized graphene. (a) Phenotypic morphology of *V. faba* seedlings between CK and G25 groups. (b) Comparison of plant height of *V. faba* seedlings between CK and G25 groups. (c) Root morphology of *V. faba* seedlings between CK and G25 groups. (d) Total root length of *V. faba* seedlings between CK and G25 groups

tographed (Fig. 2c). The total root length of the functionalized graphene-treated *V. faba* was significantly longer than that of the CK group (t = 3.661, P<0.05) (Fig. 2d). These results indicated that the application of 25 mg·L^{-1} functionalized graphene solution could promote the growth of both underground and aboveground parts in *V. faba*.

Several studies have shown that functionalized graphene at appropriate concentrations can promote the growth and development of plants. For example, Guo et al.[7] showed that functionalized graphene can increase the biomass accumulation in tomato seedlings and mature plants within a specific concentration range, while also promoting root development. Similarly, Kamal et al.[4] observed that functionalized graphene treatment could accelerate the growth rate of root and shoot of cotton and periwinkle seedlings. Ren et al.[38] demonstrated that functionalized graphene at low concentration could remove ROS in the roots of *Zea mays* seedlings, thereby weakening oxidative stress and promoting the increase of plant height. *V. faba* plants have also been studied in response to the functionalized graphene from different perspectives. For example, it has been shown that functionalized graphene can affect growth parameters, H_2O_2-decomposing enzymes and the coordination between glutathione-regenerating and glutathione-metabolizing enzymes[39-40]. In our study, we found that treatment with a 25 mg·L^{-1} solution of functionalized graphene increased the plant height and total root length of *V. faba* by 13.2% and 61.3%, respectively. This indicated that a low concentration of functionalized graphene solution can effectively promote the growth and development of *V. faba* plants.

3.3 Analysis of physical and chemical properties of rhizosphere peat soil

The effects on the physicochemical properties of rhizosphere peat soil of *V. faba* seedlings after functionalized graphene treatment are shown in Table 1. Compared with CK, the contents of total nitrogen and

Table 1　Physicochemical properties of rhizosphere peat soil of *V. faba* seedlings ($\bar{x} \pm s$)

	Concentration/(g·kg^{-1})				Concentration/(mg·kg^{-1})			pH value
	TN	TP	TK	OM	AN	AP	AK	
CK	13.70±0.00	0.41±0.00	20.55±0.92	3.57±0.08	20.41±3.13	14.54±1.33	50.74±2.23	7.42±0.18
G25	13.03±0.21*	0.52±0.00	18.06±0.20*	3.46±0.02	27.07±3.38	15.78±1.81	51.72±8.30	7.25±0.19

Note: * represents significant difference between experimental group and CK ($P < 0.05$)

total potassium in the experimental group were significantly decreased (t = 4.558 and 3.774, $P < 0.05$), while the total phosphorus content increased by 1.27 times. In addition, the experimental group had higher ammonium nitrogen, available phosphorus and available potassium contents than CK in the rhizosphere peat soil, but the differences were not significant (t = 2.768, 0.784 and 0.159, $P > 0.05$). Finally, the pH value and organic matter content of the rhizosphere peat soil in the experimental group slightly decreased with the differences not significant (t =1.397 and 1.783, $P > 0.05$).

It was observed that functionalized graphene treatment caused a decrease in the pH value of the *V. faba* rhizosphere peat soil along with an increase in the H^+ content, which was consistent with the previous conclusion[41]. The decrease in pH value can be attributed to the deprotonation of carbonyl groups on the functionalized graphene surface and the release of H^+ ions[42-43]. Baysal et al. also found that phosphate concentration increased with the increase of functionalized graphene nano-contamination, which was consistent with the increase of total phosphorus content and available phosphorus content in peat soil in this experiment. The contents of ammonium nitrogen, available phosphorus, and available potassium in the soil of the experimental group increased, which might be related to the addition of low-concentration functionalized graphene solution that can accelerate the decomposition of organic matter in *V. faba* rhizosphere peat soil and increase the content of nutrients available to plants in the soil[44].

3.4　OTU analysis of PCR-amplified bacterial 16S rRNA and fungal ITS sequences

A total of 774 067 16S rRNA raw reads and 766 134 ITS raw reads were generated from the peat soil sample DNA. After quality screening of all sequencing sequences, 653 937 16S rRNA effective tags and 624 373 ITS effective tags were obtained (Table S1, S2). According to the Shannon index curve (Fig. 3a, b) and rank abundance curve (Fig. 3c, d), the number of effective 16S rRNA sequences and ITS sequences obtained was sufficient to reflect the diversity and abundance of bacteria and fungi. These results indicated that the abundance of bacteria in the rhizosphere peat soil of *V. faba* seedlings was greater than that of fungi, and the diversity of fungi was greater than that of bacteria between the two groups.

3.5　Comparison of microbial community structure and diversity in rhizosphere peat soil of *V. faba* seedlings

Under the condition of 97% similarity, effective tags were clustered to obtain peat soil OTUs. In total, bacterial sequences were clustered to 9 144 OTUs, which belong to 39 phyla and 350 genera according to biological taxonomy (Fig. 4a). Out of these, 5 791 bacterial OTUs were in the CK group, and 5 791 OTUs were in the G25 group. There were 2 598 OTUs overlapping in these 2 groups, 3 193 unique to the CK group, and 3 353 unique to the G25 group (Fig. 4a). Regarding fungal sequences, they were clustered into 790 OTUs, which belong to 156 genera in 18 phyla (Fig. 4b). Out of these, 392 fungal OTUs were in the CK group, and 577 fungal OTUs were in the G25 group. There were 279 fungal OTUs overlapped between the 2 groups, with 213 unique OTUs in the CK group and 298 unique OTUs in the G25 group. (Fig. 4b). The PCA analysis showed significant differences in bacterial and fungal communities between the CK and G25 groups, with principal component 1 of bacterial community explaining 60.68% of the variance (Fig. 4c) and principal component 1 of the fungal community explaining 64.83% of the variance (Fig. 4d).

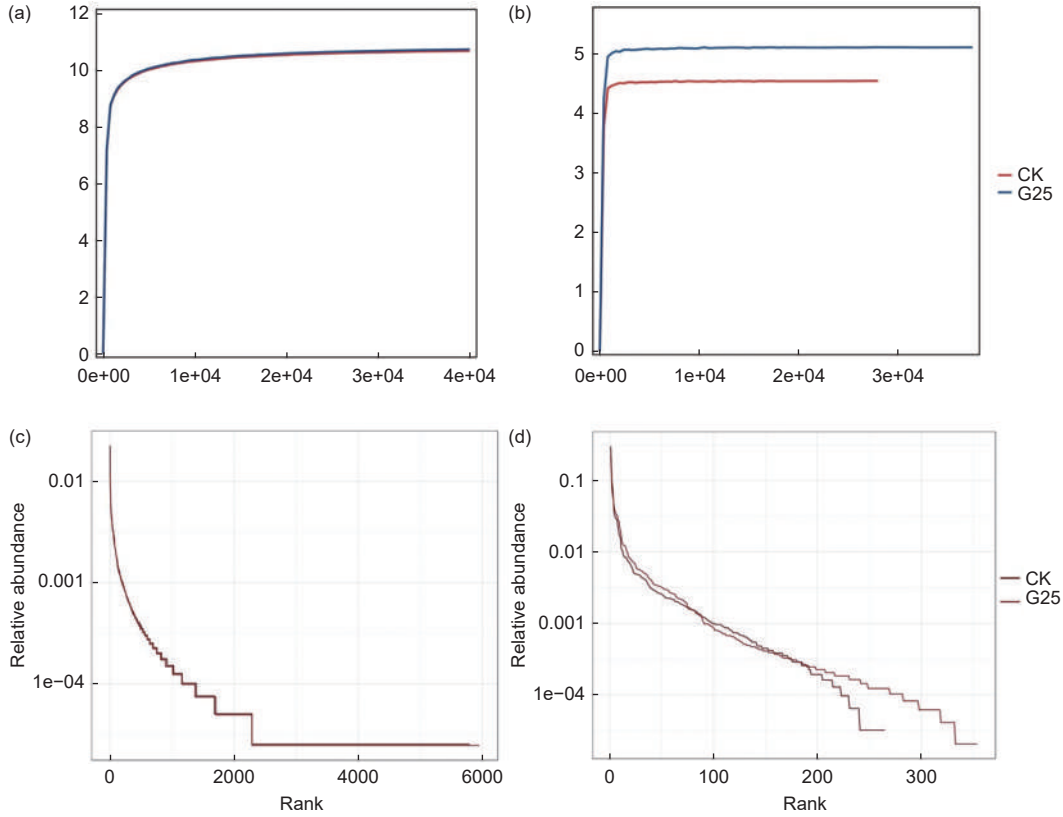

Fig. 3 Sequencing statistics and basic OTU analyses. (a) Shannon index curves of bacterial community, (b) Shannon index curves of fungal community, (c) Graded abundance curve of peat bacterial community, (d) Graded abundance curves of peat fungal community

According to the ANOSIM analysis, there was a difference in the bacterial community between the CK and G25 groups, but it was not statistically significant (Fig. 5a). However, there was a significant difference in the fungal community between the CK and G25 groups (Fig. 5b). Table 2 shows the Alpha diversity index of bacteria and fungi in the rhizosphere peat soil of *V. faba* seedlings in both CK and G25 groups, among which the Sobs, Chao1 and ACE index of bacterial and fungal communities in the G25 group were higher than those in the CK group. These indicate that the abundance, evenness and diversity of the rhizosphere bacterial and fungal communities increased in peat soil after functionalized graphene treatment.

Soil microbial community is involved in the decomposition of nutrients and the cycling of elements in soil, which is closely related to soil health[45]. Zhou et al.[12] investigated the effects of functionalized graphene on the microbial number and bacterial community in 4 different types of soils (red paddy soil, yellow loam soil, Yellowstone soil and yellow paddy soil). The results showed that the microbial number, diversity and abundance of the bacterial community in soil increased after functionalized graphene application. In this study, the structure of bacterial and fungal communities in peat soil in the experimental group did not change significantly at the phylum level, but their diversity and abundance increased slightly. Forstner et al.[14] found that functionalized graphene had less impact on the bacterial community structure in soil compared to the fungal community structure. This was consistent with the results of the similarity analysis of the two groups of bacterial and fungal community structures in our study. The overall effect of functionalized graphene on the microbial community in 25 mg·L^{-1} soil was positive, and the effect of functionalized graphene on fungal community structure was greater than that of bacteria.

3.6 Comparison of microbial composition in rhizosphere peat soil of *V. faba* seedlings

Bacterial OTU in the rhizosphere peat soil of *V. faba* seedlings derived from 39 phyla. The most

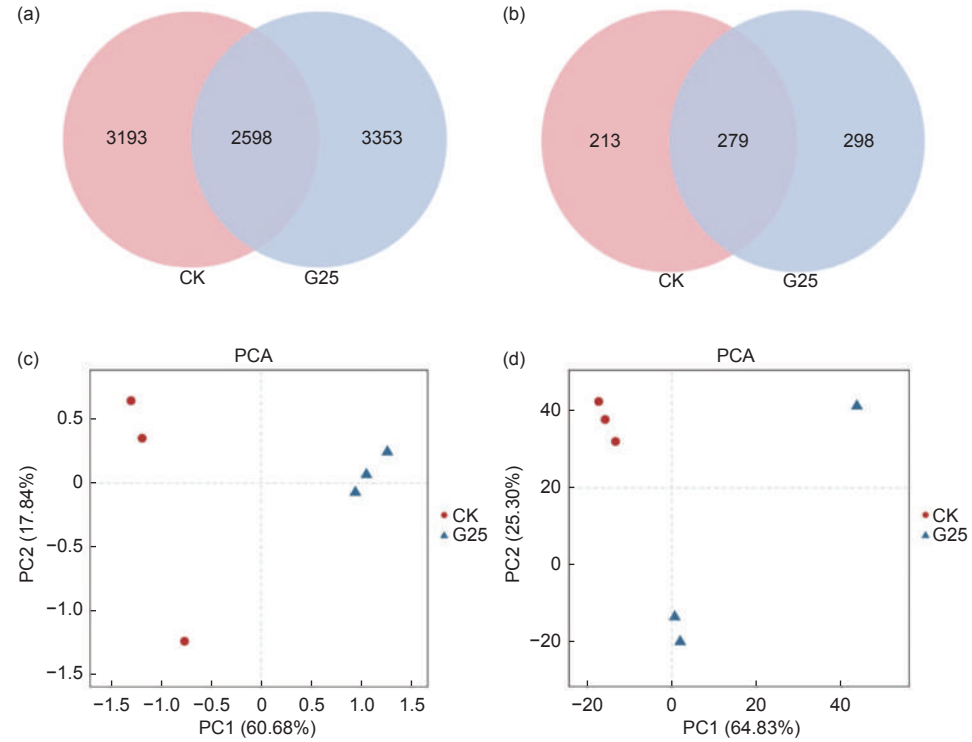

Fig. 4　Changes of microorganisms in rhizosphere peat soil. (a) Venn diagram of bacterial OTU quantity, (b) Venn diagram of fungal OTU quantity, (c) principal component analysis (PCA) of bacterial community, (d) principal component analysis (PCA) of fungal community

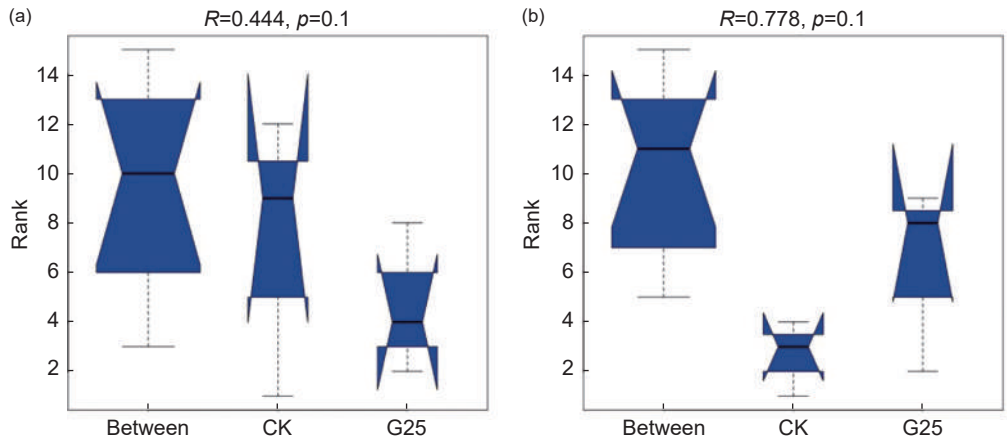

Fig. 5　Community structure similarity analyses of (a) rhizosphere peat soil bacteria and (b) fungi in CK and G25 groups

Table 2　Alpha diversity index of microorganisms in *V. faba* seedling rhizosphere peat soil ($\bar{x} \pm s$)

	Index	Sobs	Shannon	Simpson	Chao1	ACE
Bacteria	CK	6 175±151	10.69±0.06	0.9979±0.0001	6 386±123	6 745±119
	G25	6 432±385*	10.75±0.16	0.9982±0.0002	6 615±369*	6 947±368*
Fungi	CK	156±27	4.54±0.2	0.8730±0.0177	171±38	172±38
	G25	227±20*	5.10±0.93	0.8888±0.1032	243±24*	246±24*

Note: * represents significant difference between experimental group and blank group (P<0.05)

abundant bacterial OTUs belong to ten major phyla, with eight of those phyla accounting for more than 80% of the total bacterial OTUs (Fig. 6a). These eight phyla were *Proteobacteria*, *Acidobacteria*, *Bacteroidetes*, *Chloroflexi*, *Actinobacteria*, *Gemmatimonadees*, *Planctomycetes*, and *Patescibacteria* (Fig. 6a). Among these phyla, functionalized graphene treatment caused significant changes in the proportions of

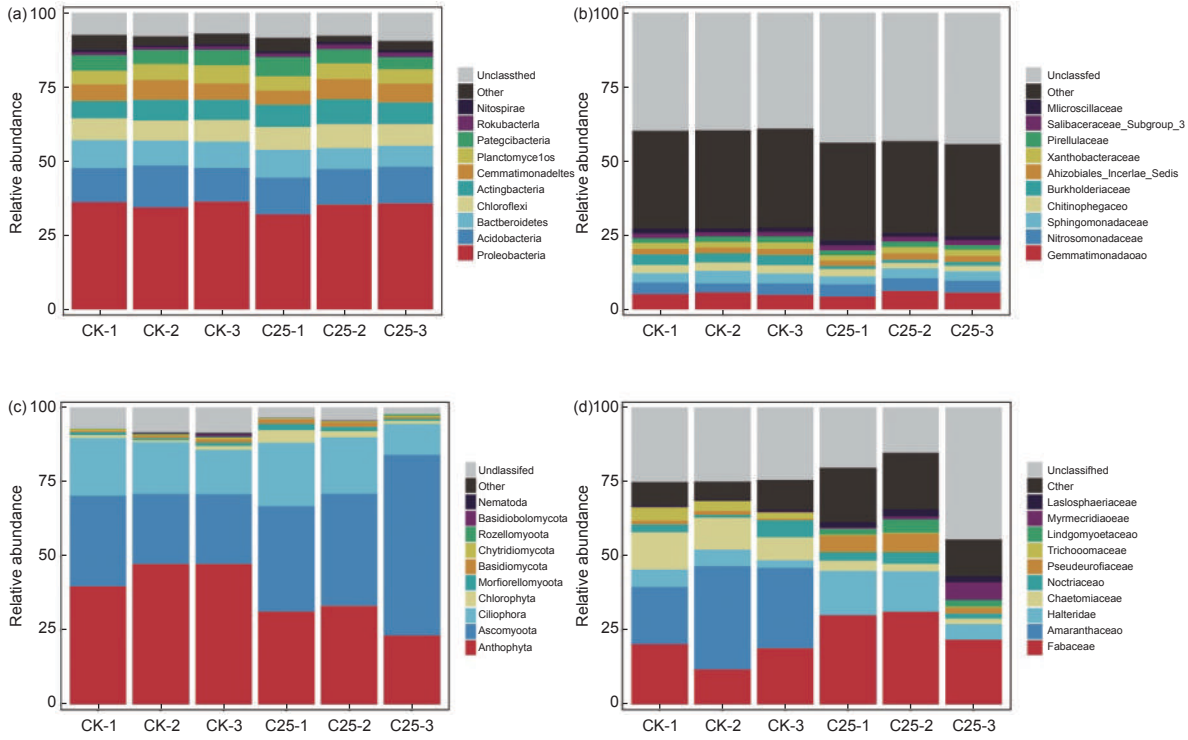

Fig. 6 Change of microbial community diversity in peat soil after functionalized graphene treatment. Relative abundance of major bacteria at (a) phylum and (b) family levels (%). Relative abundances of major fungi at (c) phylum and (d) family levels (%)

Proteobacteria, *Bacteroidetes*, *Chloroflexi*, *Actinobacteria*, *Gemmatimonadees*, and *Planctomycetes*. The proportions of *Proteobacteria*, *Bacteroidetes*, and *Planctomycetes* were significantly lower than in the G25 group, however, the levels of *Chloroflexi*, *Actinobacteria*, and *Gemmatimonadees* in the G25 group were significantly higher than in the CK group (Fig. 6a). At the family level of bacterial OTUs, differences between the 2 groups were mainly caused by changes in the levels of *Gemmatimonadaceae*, *Nitrosomonadaceae*, *Sphingomonadaceae*, *Chitinophagaceae*, and *Burkholderiaceae* (Fig. 6b). Du et al.[46] found that the abundance of bacteria related to nitrogen metabolism in the soil bacterial community was changed after functionalized graphene treatment. In our study, after treatment of *V. faba* root peat soil with functionalized graphene, the relative abundance of *hydrophagocytes* and *sphingosinomonas* (denitrifying bacteria) decreased, while the abundance of *nitrosomonas* (nitrifying bacteria) increased, indicating that functionalized graphene could change nitrogen cycling in soil by affecting the microorganisms that were involved in this process[47-48]. *Burkholderiaceae* (the family of *Hydrogenophaga*) was associated with nitrogen cycling in soil, and the relative abundance of *Burkholderiaceae* and *Sphingomonadaceae* (Denitrifying bacteria) was proportional to the total nitrogen content in the soil and inversely proportional to the ammonium nitrogen content[49]. Li et al.[50] discovered that *Brevibacillus* significantly reduced nitrogen metabolism. On the other hand, Li et al.[47] found that CL500_29_marine_group could promote nitrogen cycling. From these, it can be concluded that the application of functionalized graphene changed the rate of nitrogen cycling in soil, increased the content of nitrogen available to plants, and further to promote *V. faba* plant growth.

Fungal OTU in rhizosphere peat soil of *V. faba* seedlings derived from 18 phyla. The rhizosphere fungal community also mainly consisted of ten dominant phyla with six of those ten phyla: *Anthophyta*, *Ascomycota*, *Ciliophora*, *Chlorophyta*, *Mortierellomycota*, and *Basidiomycota*, accounting for more than 80% of the fungal OTUs (Fig. 6c). The levels of *Anthophyta*, *Ascomycota*, *Chlorophyta*, *Mortierellomycota*, and *Basidiomycota* were significantly different

between the 2 groups. Among them, *Anthophyta* level in the G25 group was significantly lower than the CK group, while *Ascomycota*, *Chlorophyta*, *Mortierellomycota*, and *Basidiomycota* levels were significantly higher than the CK group (Fig. 6c). At the family level, changes in the diversity of fungal OTUs were mainly caused by changes in the levels of *Fabaceae*, *Amaranthaceae*, *Halteriidae*, *Chaetomiaceae*, *Pseudeurotiaceae*, *Trichocomaceae*, *Lindgomycetaceae*, and *Myrmecridiaceae* (Fig. 6d).

By studying the difference of fungi in *V. faba* rhizosphere peat soil between the 2 groups, the experimental group had more dominant OTUs in fungi. Among them, *Dimorphospora* can be used as a fungal antagonist to control plant fungal diseases[51]. *Polyspora* pink is a fungal parasite, which can live in insect pests such as Coleoptera and nematodes, inhibit the growth of insect pests, and achieve the purpose of biological control[52]. *Mucor* can not only inhibit diseases, but also promote the growth of tomato[53]. *Humicola* is a filamentous fungus that degrades cellulose[54], *Podospora* is a lignocellulosic degrading bacterium[55-56]. Under the combined action of these fungi, the content of organic matter in the rhizosphere peat soil of *V. faba* decreased. The interaction force of phosphate-soluble fungi was stronger than that of phosphate-soluble bacteria[57]. *Talaromyces* was a phosphate-soluble fungus, but it was significantly inhibited by functionalized graphene, resulting in the increase of total phosphorus content in soil[58].

3.7 Differences of indicator species in rhizosphere peat soil of *V. faba* treated with functionalized graphene

The microbial community diversity of rhizosphere peat soil treated with distilled water and 25 $mg \cdot L^{-1}$ functionalized graphene was significantly different. According to LEfSe analysis in Fig. 7, the differences between the bacterial communities of the 2 groups, the abundance of *Hydrogenophaga* (CK-1.67% *vs*. G25-0.1%), *Brevibacillus* (CK-0.23% *vs*. G25-0.005%) and *Sphingomonas* (CK-2.33% *vs*. G25-1.67%) was significantly higher in the CK group than in the G25 group (Fig. 7a). The abundance of CL500_29_marine_group was 0.73% in the G25 group, which was significantly higher than in the CK group (0.97%) (Fig. 7a).

In the comparison analysis of the fungal community between the two groups, the relative abundance of three genera: *Talaromyces* (CK-11% *vs*. G25-0.67%), *Humicola* (CK-27% *vs*. G25-4%) and *Powellomyces* (CK-1.33% *vs*. G25-0.57%) in the CK group was significantly higher than that in the G25 group (Fig. 7b). However, the abundance of *Clohesyomyces* (CK-0.02% *vs*. G25-6.67%), *Leptosphaeria* (CK-0.32% *vs*. G25-0.37%), *Myrmecridium* (CK-0.25% *vs*. G25-4%), *Podospora* (CK-0.02% *vs*. G25-6.67%), *Nectria* (CK-0 *vs*. G25-0.14%), *Clonostachys* (0.44% *vs*. G25-3.63%), *Dimorphospora* (CK-1.47% *vs*. G25-6.67%), *Tausonia* (0.03% *vs*. G25-0.3%), and *Mucor* (CK-0.15% *vs*. G25-0.19%) in the G25 group was significantly higher than that in the CK group (Fig. 7b).

3.8 Redundancy analysis of microbial community composition and physicochemical properties

To investigate the relationship between the physicochemical properties of rhizosphere peat soil and microbial communities, distance-based redundancy was analyzed at the phylum and family taxonomic levels, respectively. The results of redundancy analysis of bacterial community diversities and physicochemical properties are shown in Fig. 8 (a, b). At the phylum taxonomic level, the first and second coordinates explained 54.81% and 27.66% of the total variation between bacterial community composition and physicochemical properties of rhizosphere peat soil, respectively (Fig. 8a). In detail, *Planctomycetes*, *Proteobacteria* and *Bacteroidetes* were positively correlated with TN. *Bacteroidetes* and *Nitrospirae* were positively correlated with pH values. *Chloroflexi*, *Acidobacteria* and *Actinobacteria* were positively correlated with AP. *Rokubacteria*, *Proteobacteria*, *Gemmatimonadetes* and *Actinobacteria* were positively correlated with OM and AK (Fig. 8a). Among them, pH value was the main factor affecting the change of rhizosphere bacterial community composition (F=1.3, P=0.1). In addition, at the family taxonomic level, the

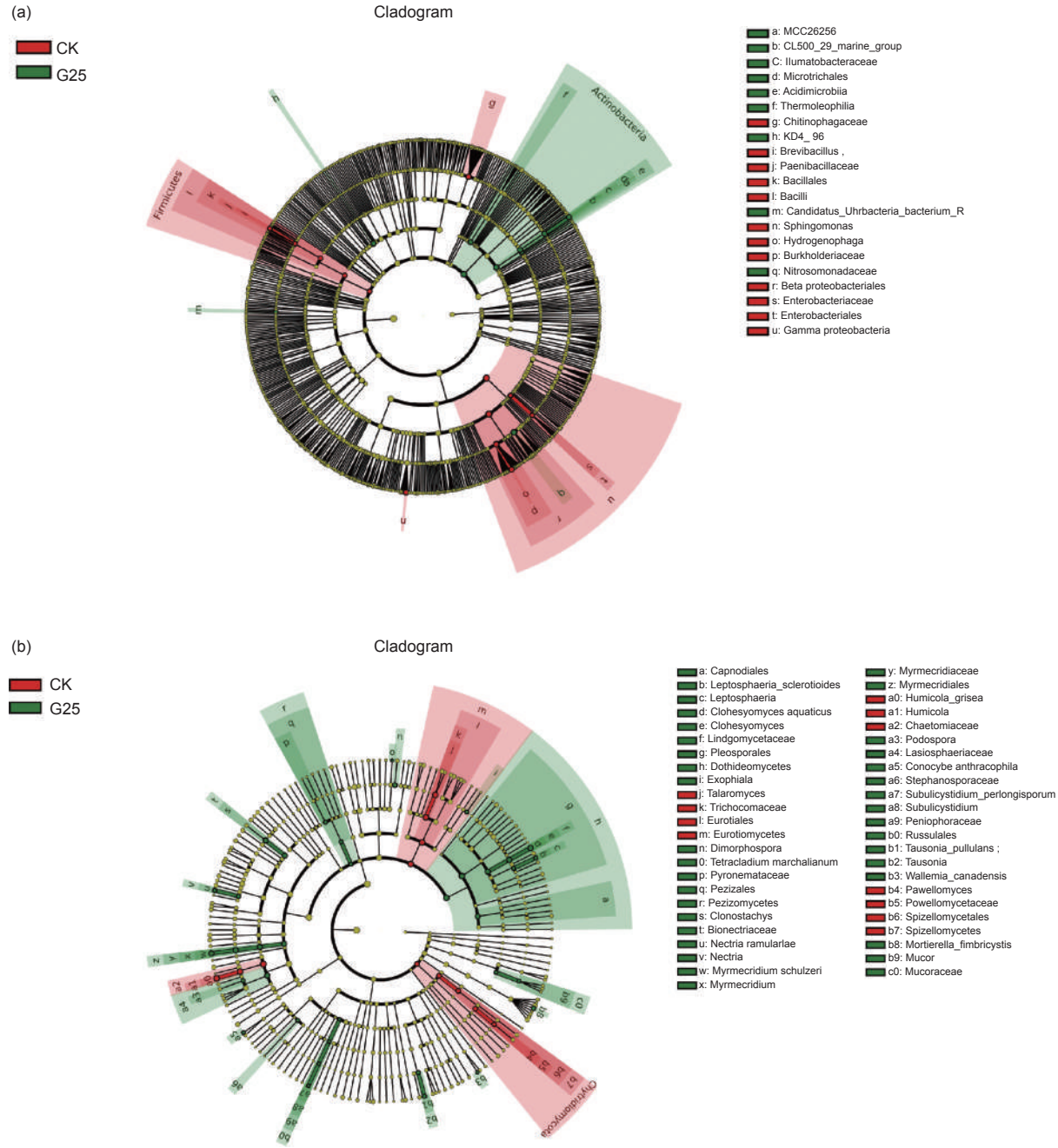

Fig. 7 LDA effect size lineages of LEfSe for (a) bacteria and (b) fungi (LDA Score<3). In the concentric circles of the clade, each circle from the inside out represents the classification level of phylum to species. The circle on the ring represents a classification at this classification level, and the relative abundance of this classification is positively correlated with the size of the circle. Coloring principle: all species without significant difference are shown yellow, CK group is red, G25 group is green

first and second coordinates explained 68.19% and 22.76% of the total variation between the top ten dominant families of bacterial communities and the physicochemical properties, respectively (Fig. 8b). *Sphingomonadaceae*, *Gemmatimonadaceae* and *Chitinophagaceae* were positively correlated with OM. *Chitinophagaceae*, *Burkholderiaceae*, *Sphingomonadaceae* and *Pyriformaceae* were positively correlated with TN. *Gemmatimonadaceae* and *Nitrosomonadaceae* were positively correlated with TP, AP and AN. According to these results of the distribution of bacterial species in rhizosphere peat soil, TP was the primary factor affecting the change of rhizosphere bacterial community composition (F=6.9, P= 0.078).

The results of the redundancy analysis of fungal community diversities and physicochemical proper-

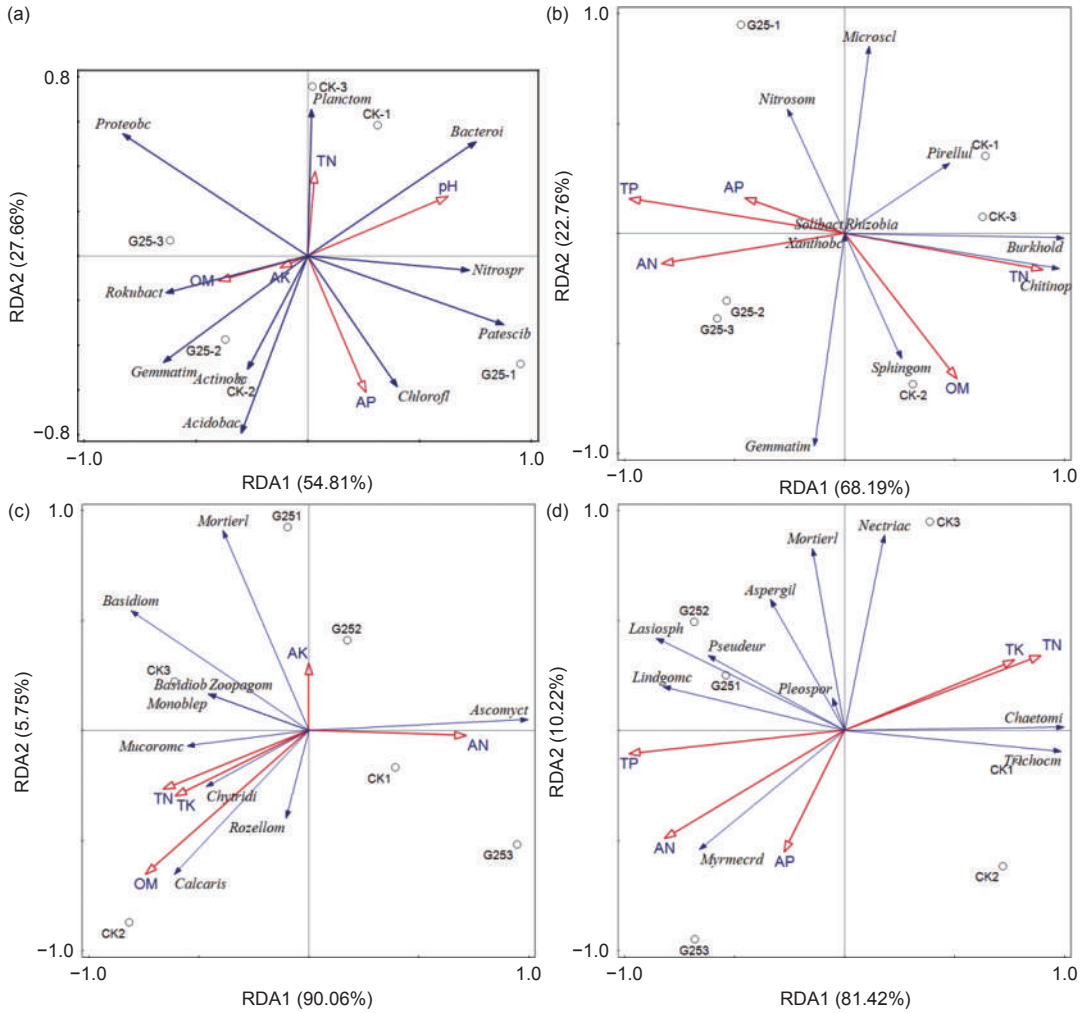

Fig. 8　Distance-based redundancy analysis (RDA) of (a, b) bacterial and (c, d) fungal communities and soil physicochemical properties. Arrows indicate different environmental factors and species. Small circles indicate groups. When the included Angle of the arrow is acute, it indicates that the two are positively correlated. When the Angle between the arrows is obtuse, the two are negatively correlated

ties were shown in Fig. 8c, d. At the phylum taxonomic level, the first and second coordinates explained 90.06% and 5.75% of the total variation between the fungal community composition and physicochemical properties (Fig. 8c). Ascomycota was positively correlated with AN, while *Calcarisporiellomycota*, *Rozellomycota*, *Chytridiomycota* and *Mucoromycota* were positively correlated with OM, TN and TK. After the interpretation of environmental factors, OM was found to be the primary factor affecting the change of rhizosphere fungal community composition (F=4.2, P=0.094). At the family taxonomic level, the first and second coordinates explained 81.42% and 10.22% of the total variation between the top ten dominant families of the fungal community and the physicochemical properties of rhizosphere peat soil, respectively (Fig. 8d). There was a positive correlation between *Chaetomiaceae*, *Nectriaceae* and *Trichocomaceae* with TK and TN. *Myrmecridiaceae*, *Lindgomycetaceae* and *Chaetomiaceae* were positively correlated with TP, AN and AP. According to the influence of environmental factors on the distribution of fungal species in rhizosphere peat soil, TP was the main factor affecting the change of rhizosphere fungal community composition (F=13.5, P=0.078). Through redundancy analysis, it was found that the correlation between fungal community composition and physicochemical properties was higher than that of bacteria after functionalized graphene treatment.

These results of the redundancy analysis showed that *Trichocomaceae* was negatively correlated with total phosphorus content, indicating that functional-

ized graphene application reduced the abundance of phospho-soluble fungi, slowed down the phospho-soluble effect, and changed the rate of phosphorus cycling in soil. There was a significant correlation between phosphorus nutrient content and plant yield[59-60]. Thus, it was necessary to extend the treatment time of *V. faba* seedlings with functionalized graphene to study the relationship between *V. faba* yield and soil phosphorus solubilizing bacteria or fungi contents. Finally, our study demonstrated the relationship between functionalized graphene-rhizosphere soil microbe-physicochemical properties, and explained the microbiome mechanism of functionalized graphene in promoting *V. faba* plant growth and development.

4 Conclusions

In this study, *V. faba* roots were treated with 0 and 25 $mg \cdot L^{-1}$ functionalized graphene solutions. The results showed that functionalized graphene had a significant effect on the richness and diversity of bacteria and fungi in *V. faba* rhizosphere peat soil. And the effect of functionalized graphene on the fungal community is greater than that on the bacterial community. After the application of the functionalized graphene, the content of bacteria that promote soil nitrogen cycling and cellulose decomposition increased, further promoting the growth of *V. faba* seedlings. In the fungal community composition, functionalized graphene significantly decreased the abundance of phosphate-soluble fungi, which may have an impact on the subsequent reproductive development of *V. faba* seedlings. Further studies are needed to gain a better understanding of this impact.

Acknowledgements

This work was supported by the National Natural Science Foundation of China (52071192), the Engineering Research Center of Coal-Based Ecological Carbon Sequestration Technology of the Ministry of Education, the Scientific and Technological Innovation Programs of Higher Education Institutions in Shanxi (2023L263, 2022L426), the Shanxi 1331 Project Foundation for Graphene Industrialization Application Technology of Collaborative Innovation Center, and Shanxi New Carbon Functional Materials Engineering Research Center.

References

[1] Ojha R P, Lemieux P A, Dixon P K, et al. Statistical mechanics of a gas-fluidized particle[J]. Nature, 2004, 427(6974): 521-523.

[2] Kabiri S, Degryse F, Tran D N H, et al. Graphene oxide: A new carrier for slow release of plant micronutrients[J]. ACS Applied Materials & Interfaces, 2017, 9(49): 43325-43335.

[3] Wang X, Xie H, Wang Z, et al. Graphene oxide as a multifunctional synergist of insecticides against lepidopteran insect[J]. Environmental Science: Nano, 2019, 6(1): 75-84.

[4] Pandey K, Anas M, Hicks V K, et al. Improvement of commercially valuable traits of industrial crops by application of carbon-based nanomaterials[J]. Scientific Reports, 2019, 9: 19358.

[5] Chen Z, Zhao J, Qiao J, et al. Graphene-mediated antioxidant enzyme activity and respiration in plant roots[J]. ACS Agricultural Science & Technology, 2022, 2(3): 646-660.

[6] Chen Z, Zhao J, Song J, et al. Influence of graphene on the multiple metabolic pathways of *Zea mays* roots based on transcriptome analysis[J]. PloS ONE, 2021, 16(1): e0244856.

[7] Guo X, Zhao J, Wang R, et al. Effects of graphene oxide on tomato growth in different stages[J]. Plant Physiol Biochem, 2021, 162: 447-455.

[8] Zhang X, Cao H, Zhao J, et al. Graphene oxide exhibited positive effects on the growth of *Aloe vera* L[J]. Physiol Mol Biol Plants, 2021, 27(4): 815-824.

[9] Ren C, Liu K, Dou P, et al. The changes in soil microorganisms and soil chemical properties affect the heterogeneity and stability of soil aggregates before and after grassland conversion[J]. Agriculture, 2022, 12(2): 307.

[10] Ru J, Chen G, Liu Y, et al. Graphene oxide influences bacterial community and soil environments of Cd-polluted Haplic Cambisols in Northeast China[J]. Journal of Forestry Research, 2020, 32(4): 1699-1711.

[11] Zhou Q, Li D, Wang T, et al. Leaching of graphene oxide nanosheets in simulated soil and their influences on microbial communities[J]. J Hazard Mater, 2021, 404(Pt A): 124046.

[12] Rong Y, Wang Y, Guan Y, et al. Pyrosequencing reveals soil enzyme activities and bacterial communities impacted by graphene and its oxides[J]. Journal of Agricultural and Food Chemistry, 2017, 65(42): 9191-9199.

[13] Chung H, Kim M J, Ko K, et al. Effects of graphene oxides on soil enzyme activity and microbial biomass[J]. Sci Total Environ, 2015, 514: 307-313.

[14] Forstner C, Orton T G, Skarshewski A, et al. Effects of graphene oxide and graphite on soil bacterial and fungal diversity[J]. Science of the Total Environment, 2019, 671: 140-148.

[15] Insam H. Developments in soil microbiology since the mid 1960s[J]. Geoderma, 2001, 100(3-4): 389-402.

[16] Pang W, Crow W T, Luc J E, et al. Comparison of water

displacement and WinRHIZO software for plant root parameter assessment[J]. Plant Dis, 2011, 95(10): 1308-1310.

[17] Liu Z H, Chen Z W, Zhao J G, et al. Effects of graphene on the growth and development of *Vicia faba* L[J]. Journal of Capital Normal University (Natural Science Edition), 2020, 41(05): 33-39.

[18] MEP(China). Soil - determination of total nitrogen (KJELDAHL method): HJ 717-2014[S]. In. : Beijing: Standards Press of China, 2014.

[19] MOA(PRC). Soil-determination of total phosphorus: NY/T 88-1988[S]. In Beijing: Standards Press of China, 1988.

[20] MOA(PRC). Soil-determination of total potassium: NY/T 87-1988[S]. In Beijing: Standards Press of China, 1988.

[21] Magoc T, Salzberg S L. FLASH: fast length adjustment of short reads to improve genome assemblies[J]. Bioinformatics, 2011, 27(21): 2957-2963.

[22] Bolger A M, Lohse M, Usadel B. Trimmomatic: a flexible trimmer for Illumina sequence data[J]. Bioinformatics, 2014, 30(15): 2114-2120.

[23] Edgar R C. UPARSE: highly accurate OTU sequences from microbial amplicon reads[J]. Nature Methods, 2013, 10(10): 996-998.

[24] Bokulich N A, Subramanian S, Faith J J, et al. Quality-filtering vastly improves diversity estimates from Illumina amplicon sequencing[J]. Nature Methods, 2013, 10(1): 57-59.

[25] Wang Q, Garrity G M, Tiedje J M, et al. Naive bayesian classifier for rapid assignment of rRNA sequences into the new bacterial taxonomy[J]. Applied and Environmental Microbiology, 2007, 73(16): 5261-5267.

[26] Quast C, Pruesse E, Yilmaz P, et al. The SILVA ribosomal RNA gene database project: Improved data processing and web-based tools[J]. Nucleic Acids Research, 2012, 41(D1): D590-D596.

[27] Abarenkov K, Nilsson R H, Larsson K H, et al. The UNITE database for molecular identification of fungi - recent updates and future perspectives[J]. New Phytologist, 2010, 186(2): 281-285.

[28] Chen H, Boutros P C. VennDiagram: A package for the generation of highly-customizable Venn and Euler diagrams in R[J]. BMC Bioinformatics, 2011, 12(1): 1-7.

[29] Caporaso J G, Kuczynski J, Stombaugh J, et al. QIIME allows analysis of high-throughput community sequencing data[J]. Nature Methods, 2010, 7(5): 335-336.

[30] Segata N, Izard J, Waldron L, et al. Metagenomic biomarker discovery and explanation[J]. Genome Biol, 2011, 12(6): R60.

[31] Furby K A, Bouwmeester J, Berumen M L. Susceptibility of central red sea corals during a major bleaching event[J]. Coral reefs, 2013, 32(2): 505-513.

[32] Ginestet C. ggplot2: Elegant graphics for data analysis[J]. Journal of the Royal Statistical Society Series a-Statistics in Society, 2011, 174: 245-245.

[33] Xi S, Gao X W, Cheng X M, et al. Deposition of MnO_2 on KOH-activated laser-produced graphene for a flexible planar micro-supercapacitor[J]. New Carbon Materials, 2023, 38(5): 913-924.

[34] Zhu C, Dong X, Mei X, et al. Direct laser writing of MnO_2 decorated graphene as flexible supercapacitor electrodes[J]. Journal of Materials Science, 2020, 55(36): 17108-17119.

[35] Lamberti A, Perrucci F, Caprioli M, et al. New insights on laser-induced graphene electrodes for flexible supercapacitors: tunable morphology and physical properties[J]. Nanotechnology, 2017, 28(17): 174002.

[36] Aziz M, Abdul Halim F S, Jaafar J. Preparation and characterization of graphene membrane electrode assembly[J]. Jurnal Teknologi, 2014, 69(9): 11-14.

[37] Guo Y F, Zhang H T, Liu Y W, et al. Molecular-scale grinding of uniform small-size graphene flakes for use as lubricating oil additives[J]. New Carbon Materials, 2023, 38(5): 954-963.

[38] Ren W, Chang H, Teng Y. Sulfonated graphene-induced hormesis is mediated through oxidative stress in the roots of maize seedlings[J]. Science of the Total Environment, 2016, 572: 926-934.

[39] Anjum N A, Singh N, Singh M K, et al. Single-bilayer graphene oxide sheet impacts and underlying potential mechanism assessment in germinating faba bean (Vicia faba L.)[J]. Science of The Total Environment, 2014, 472: 834-841.

[40] Anjum N A, Singh N, Singh M K, et al. Single-bilayer graphene oxide sheet tolerance and glutathione redox system significance assessment in faba bean (Vicia faba L.)[J]. Journal of Nanoparticle Research, 2013, 15(7): 1770.

[41] Baysal A, Saygin H, Ustabasi G S. Risks of graphene nanomaterial contamination in the soil: evaluation of major ions[J]. Environ Monit Assess, 2020, 192(10): 622.

[42] Wang Z, Shen C, Du Y, et al. Influence of phosphate on deposition and detachment of TiO_2 nanoparticles in soil[J]. Frontiers of Environmental Science & Engineering, 2019, 13(5): 1-11.

[43] He K, Chen G, Zeng G, et al. Stability, transport and ecosystem effects of graphene in water and soil environments[J]. Nanoscale, 2017, 9(17): 5370-5388.

[44] Song J, Cao K, Duan C, et al. Effects of graphene on Larix olgensis seedlings and soil properties of Haplic Cambisols in Northeast China[J]. Forests, 2020, 11(3): 258.

[45] Kennedy A C, Smith K. Soil microbial diversity and the sustainability of agricultural soils[J]. Plant and soil, 1995, 170(1): 75-86.

[46] Du J, Hu X, Zhou Q. Graphene oxide regulates the bacterial community and exhibits property changes in soil[J]. RSC Advances, 2015, 5(34): 27009-27017.

[47] Jianzhu L, Jie H, Pengfei Z, et al. Influence on water quality and microbial diversity in fish pond by Ipomoea aquatica floating-bed[J]. China Environmental Science, 2016, 36(10): 3071-3080.

[48] Zhang H, Wang Y, Huang T, et al. Mixed-culture aerobic anoxygenic photosynthetic bacterial consortia reduce nitrate: Core species dynamics, co-interactions and assessment in raw water of reservoirs[J]. Bioresource Technology, 2020, 315: 123817.

[49] Van V T, Berge O, Ke S N, et al. Repeated beneficial effects of rice inoculation with a strain of *Burkholderia vietnamiensis* on early and late yield components in low fertility sulphate acid soils of Vietnam[J]. Plant and Soil, 2000, 218(1): 273-284.

[50] Li C, Shi W, Wu D, et al. Biocontrol of potato common scab by *Brevibacillus laterosporus* BL12 is related to the reduction of pathogen and changes in soil bacterial community[J]. Biological Control, 2021, 153: 104496.

[51] Yang D, Plante F, Bernier L, et al. Evaluation of a fungal

antagonist, *Phaeotheca dimorphospora*, for biological control of tree diseases[J]. Canadian Journal of Botany, 1993, 71(3): 426-433.

[52] Yuan C, Wang X, Asemoloye M D, et al. First record of Clonostachys rosea as entomopathogenic fungus of Coleoptera in China[J]. Plant Biosystems, 2021, 155(6): 1240-1246.

[53] Nartey L K, Pu Q, Zhu W, et al. Antagonistic and plant growth promotion effects of Mucor moelleri, a potential biocontrol agent[J]. Microbiological Research, 2022, 255: 126922.

[54] Steindorff A S, Serra L A, Formighieri E F, et al. Insights into the Lignocellulose-degrading enzyme system of Humicola grisea var. thermoidea based on genome and transcriptome analysis[J]. Microbiology spectrum, 2021, 9(2): e01088-01021.

[55] Dicko M, Ferrari R, Tangthirasunun N, et al. Lignin degradation and its use in signaling development by the coprophilous ascomycete *Podospora anserina*[J]. Journal of Fungi, 2020, 6(4): 278.

[56] Van Erven G, Kleijn A F, Patyshakuliyeva A, et al. Evidence for ligninolytic activity of the ascomycete fungus *Podospora anserina*[J]. Biotechnology for biofuels, 2020, 13(1): 1-12.

[57] Luo L, Ye H, Zhang D, et al. The dynamics of phosphorus fractions and the factors driving phosphorus cycle in Zoige Plateau peatland soil[J]. Chemosphere 2021, 278: 130501.

[58] Qi Z, Jihua W, Haichao S, et al. Screening, compounding and embedding immobilization effect of soybean rhizosphere phosphate solubilizing fungi[J]. Molecular Plant Breeding, 2019, 17(10): 3353-3363.

[59] Smith M R, Dinglasan E, Veneklaas E, et al. Effect of drought and low P on yield and nutritional content in common bean[J]. Frontiers in Plant Science, 2022, 13: 814325-814325.

[60] Cao J F, Chen Z W, Wang L Y, et al. Graphene enhances artemisinin production in traditional medicinal plant *Artemisia annua* via dynamic physiological progress and miRNA regulation[J]. Plant Communications, 2024, 5(3): 100742.